Contents lists available at ScienceDirect

Applied Catalysis B: Environmental

Lean NO$_x$ reduction over Ag/alumina catalysts via ethanol-SCR using ethanol/gasoline blends

Fredrik Gunnarsson [a], Josh A. Pihl [b], Todd J. Toops [b], Magnus Skoglundh [a], Hanna Härelind [a,*]

[a] Competence Centre for Catalysis, Department of Chemistry and Chemical Engineering, Chalmers University of Technology, SE-412 96 Göteborg, Sweden
[b] Fuels, Engines, and Emissions Research Center, Oak Ridge National Laboratory, 2360 Cherahala Blvd., Knoxville, TN 37932, United States

ARTICLE INFO

ABSTRACT

This study focuses on the activity for lean NO$_x$ reduction over sol-gel synthesized silver alumina (Ag/Al$_2$O$_3$) catalysts, with and without platinum doping, using ethanol (EtOH), EtOH/C$_3$H$_6$ and EtOH/gasoline blends as reducing agents. The effect of ethanol concentration, both by varying the hydrocarbon-to-NO$_x$ ratio and by alternating the gasoline concentration in the EtOH/gasoline mixture, is investigated. High activity for NO$_x$ reduction is demonstrated for powder catalysts for EtOH and EtOH/C$_3$H$_6$ as well as for monolith coated catalysts (EtOH and EtOH/gasoline). The results show that pure Ag/Al$_2$O$_3$ catalysts display higher NO$_x$ reduction and lower light-off temperature as compared to the platinum doped samples. The 4 wt.% Ag/Al$_2$O$_3$ catalyst displays 100% reduction in the range 340–425 °C, with up to 37% selectivity towards NH$_3$. These results are also supported by DRIFTS (Diffuse reflection infrared Fourier transform spectroscopy) experiments. The high ammonia formation could, in combination with an NH$_3$-SCR catalyst, be utilized to construct a NO$_x$ reduction system with lower fuel penalty *cf. stand alone* HC-SCR. In addition, it would result in an overall decrease in CO$_2$ emissions.

© 2016 Elsevier B.V. All rights reserved.

1. Introduction

Stringent emission legislations and increasing awareness of climate changes are strong drivers for the use of sustainable fuels and for the implementation of more energy efficient engines within the transportation sector. These engines use higher oxygen concentration in the combustion chamber, *i.e.* higher air-to-fuel (A/F) ratios, which results in more complete combustion. This leads to decreased fuel consumption and thus the emissions of anthropogenic CO$_2$ are lowered, compared to engine concepts based on stoichiometric combustion. The emission restrictions of today consider particulate matter (PM) and nitrogen oxides (NO$_x$) in particular. Emissions of NO$_x$ are hazardous to the environment, acting as a source for ground level ozone, acid rain and eutrophication, as well as being directly harmful to humans [1,2]. The legislated maximum emission levels of NO$_x$ for cars have been decreased from 0.97 g/km (HC + NO$_x$) in 1992 (Euro I), to 0.06 g/km (only NO$_x$) in the Euro VI levels, implemented in 2013/2014 [3]. Solving the problem of NO$_x$ emission abatement is therefore of crucial importance. Conventionally, NO$_x$ emissions from stoichiometric combustion are

reduced by the three-way-catalyst (TWC). However, the lean environment in the exhaust gas from the more fuel efficient lean-burn engine systems obstructs the NO$_x$ reduction in the TWC, as these systems operate at high A/F ratios [4]. One possible technique circumventing this problem, is selective catalytic reduction of NO$_x$ using either hydrocarbons, *i.e.* fuel or derivatives from the fuel, (HC-SCR), or urea which decomposes to ammonia (NH$_3$-SCR), as the reducing agent [5].

Silver-alumina (Ag/Al$_2$O$_3$) is among the most promising catalysts for HC-SCR, displaying high NO$_x$ reduction for a variety of hydrocarbons, including fossil fuels and bio-fuels [6,7]. One drawback with the Ag/Al$_2$O$_3$ system has been that the system requires relatively high temperatures to achieve high catalytic activity. Meanwhile, as the energy-efficiency in engines increases, the exhaust gas temperature decreases. Many new engine designs also include heat recovery systems, which decrease the temperature of the exhaust gas reaching the catalyst even further. Nevertheless, the active temperature window for HC-SCR over Ag/Al$_2$O$_3$ using non-oxygenated hydrocarbons may be shifted towards lower temperatures, provided a small amount of hydrogen is introduced to the exhaust gas [8]. The addition of hydrogen further results in an over-all increase in the NO$_x$ reduction, where the highest activity generally has been reported over Ag/Al$_2$O$_3$ catalysts containing 2 wt.% Ag [9,10]. The added hydrogen does however increase the fuel-penalty, as it is produced from on-board fuel-

---

* Corresponding author.
E-mail address: hanna.harelind@chalmers.se (H. Härelind).

reforming. Recently Kannisto et al. [11] have shown that hydrogen levels as low as 1000 ppm result in a fuel penalty of about 2%, compared to 0.5% for urea-SCR. Hence, if the need to add hydrogen could be avoided, the efficiency of the engine system could be kept higher. It has been shown that a remarkably high NO_x reduction can be achieved when utilizing ethanol (EtOH) as reducing agent without the addition of hydrogen [12]. Although ethanol was one of the first fuels for passenger car engines it was discontinued in favor of gasoline in the early 1900's. It has however made its way back into the present fuel range, with almost all of the gasoline sold today containing up to 10% EtOH. Many countries also offer the choice of E85, with up to 85% EtOH and 15% gasoline (legislated range in the US is between 50 and 84% EtOH). In addition to high NO_x reduction, EtOH-SCR has also been shown to produce high amounts of NH_3 with a selectivity up to 45% [12,13]. Owing to the high levels of NH_3 downstream of the Ag/Al_2O_3 catalyst, the system displays further possibilities. NH_3-SCR is currently the most used NO_x abatement system in heavy-duty applications, with an exceptionally high NO_x reduction over a wide temperature window; however, adding the complexity, weight and cost of the NH_3-SCR system, with an additional liquid reductant (urea/H_2O solution) tank, to a car is not desirable. As the EtOH-SCR process has shown a high selectivity to NH_3, a combined system with an up-stream Ag-alumina catalyst followed by an NH_3-SCR catalyst could improve the NO_x reduction even further and lower the fuel penalty [13].

The main reactions in HC-SCR are the NO_x reduction, facilitated by the hydrocarbon reductant, and the competing combustion reaction, where the hydrocarbon is oxidized by molecular oxygen. To favor the desired reaction and to achieve high performance at low temperatures, the hydrocarbon needs to be activated, i.e. partially oxidized, before reacting with the NO_x to form N_2 [14,15]. However, as ethanol is an oxygenated hydrocarbon, this process might not be required. Although the complete reaction mechanism is still under debate, several active sites are likely involved e.g. silver ions, small silver clusters and larger metallic silver particles [16–18]. The oxidation potential of the oxidation sites, of crucial importance for non-oxygenated hydrocarbons, might not play as an important role for EtOH-SCR. The sol-gel synthesized catalysts have shown a higher ratio of small Ag-clusters and Ag-ions compared to catalysts prepared via incipient wetness, thought to play a key role in the NO_x reduction reaction [19,20]. Previous studies [11,19] indicate that trace amounts of platinum incorporated in the silver-alumina catalyst can increase the maximum NO_x reduction and, at the same time, decrease the onset temperature of the HC-SCR reaction with non-oxygenated hydrocarbons. It has also been suggested that addition of trace amounts of platinum can increase the amount of reactive HC-species on the catalyst surface and/or increase the oxidation properties of the active sites [19].

The objective of the present study is to investigate the effect of silver loading and the role of platinum doping for the lean NO_x reduction over silver-alumina catalysts using ethanol and ethanol/gasoline blends, with special focus on the low-temperature regime relevant for lean-burn gasoline and/or ethanol applications. In addition, in situ infrared spectroscopy is utilized to follow the evolution of surface species during reaction as a function of reducing agent and catalyst surface.

2. Experimental methods

2.1. Sample preparation

Ag/Al_2O_3 samples were prepared by a sol-gel based method including freeze-drying [21], with a nominal silver loading of 2 and 4 wt.%. In addition, two 2 wt.% Ag samples were prepared with addition of 100 and 500 ppm platinum. The catalysts are denoted as:

Ag(silver loading in%) Pt(platinum doping in ppm), i.e. the sample containing 2 wt.% Ag and 100 ppm Pt is denoted Ag2Pt100. The alumina precursor (aluminum isopropoxide, >98%, Aldrich) was added to milli-Q water and heated to 82 °C during vigorous stirring. Subsequently, the silver precursor ($AgNO_3$, >99%, Sigma), and for the Pt doped samples a platinum precursor ($Pt(NO_3)_2$, Heraeus), were added. The pH was adjusted to 4.5 by addition of HNO_3 (10%, Fluka), resulting in the formation of a sol. The sol was stirred for 12 h, after which a major part of the solvent was removed using a heated vacuum system. The resulting gel was freeze-dried in order to preserve the microporous structure of the formed aluminum oxy-hydroxide and to minimize the migration of silver in the pores during the drying process. The resulting cryogels were calcined in air at 600 °C for 6 h and finally ground to a fine powder. The sol-gel samples have previously been characterized in connection to HC-SCR using n-octane and bio-diesel (NExBTL) [20,22], showing a high repeatability in particle size distribution and specific surface area [19].

The Ag2Pt100 and Ag4 samples were subsequently wash-coated onto ceramic cordierite monolith substrates (400 cpsi, L = 50 mm, OD = 20 mm). A wash-coat slurry was prepared with 20 wt.% dry content, where the dry part consisted of 20 wt.% AlOOH-binder (Disperal P2, Sasol) and 80 wt.% powder catalyst. The solvent consisted of 50 wt.% H_2O and 50 wt.% ethanol. The monoliths were submerged in the slurry, dried at 90 °C and then subjected to a fast calcination at 600 °C in air for 2 min. The wash-coating procedure was repeated until sufficient amount of wash-coat (20 wt.% of the final weight) had been deposited, where after the coated monolith samples were calcined in air (600 °C, 3 h).

2.2. Flow-reactor experiments

The catalytic performance of the Ag/Al_2O_3 samples for lean NO_x reduction was initially evaluated in a packed bed gas flow microreactor [23,24] at transient conditions using pure EtOH and an 1:1 blend of EtOH and C_3H_6, as the reducing agent. The flow-reactor consisted of an U-shaped quartz tube (ID = 6 mm), placed in a furnace. The powder catalyst (100 mg) was kept in place by two small quartz wool plugs placed just above the bend in the quartz reactor U-tube and on top of the catalyst bed [24,25]. The temperature was measured using a type K thermocouple, placed in the center of the catalyst bed, and controlled by PID-controllers. The inlet gas composition (500 ppm NO, 10% O_2 and Ar_{bal}) was controlled by separate mass flow controllers and the outlet gas composition was analyzed using a mass spectrometer and two NO_x analyzers. Water (corresponding to 5%) was introduced by saturating a nitrogen flow through a heated water bath and the ethanol (corresponding to 1500 ppm) was introduced to the gas feed via a chilled water bath (1500 ppm EtOH, C/N = 6). The gas flow was set at a W/F = 0.25 (GHSV = 50 000 h^{-1}).

The catalyst samples were initially conditioned in 10% oxygen (Ar_{bal}) at 500 °C for 2 h, where after the reactants were introduced and the temperature was linearly decreased to 150 °C. The C/N molar ratio was kept at 6 for the duration of the experiment, corresponding to a C_1-concentration of 3000 ppm. The NO and total NO_x concentrations were measured using NO_x chemiluminescense detectors (California Analytical Instruments Model 400-HCLD) and the NO_x reduction was calculated in accordance with Eqs. (1) and (2).

$$NO_x = NO + NO_2 \tag{1}$$

$$NO_x\,reduction\,(\%) = 100 \times \frac{\left(NO_{x,in} - NO_{x,out}\right)}{NO_{x,in}} \tag{2}$$

Furthermore, the two wash-coated monolith samples (Ag2Pt100 and Ag4) were evaluated in a synthetic bench-scale gas flow reactor at steady-state conditions. The samples were evalu-
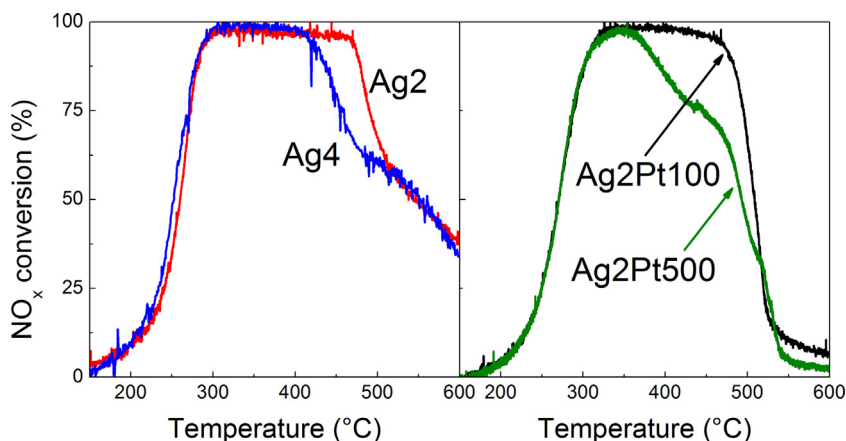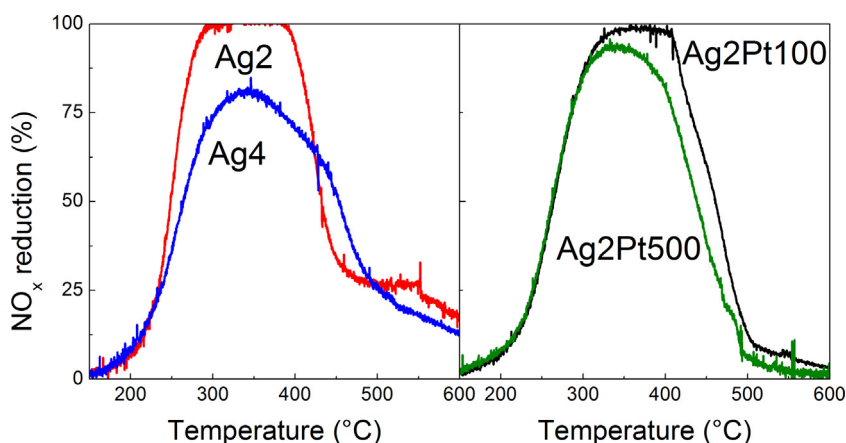
Fig. 1. NO$_x$ reduction results from fixed powder bed micro-reactor experiments using pure EtOH as reducing agent at a C/N molar ratio of 6. Left panel: Ag2 (red) and Ag4 (blue), right panel: Ag2Pt100 (black) and AgPt500 (green). Inlet gas composition: 500 ppm NO, 10 vol.% O$_2$, 5 vol.% H$_2$O, and N$_2$ balance; GHSV = 50,000 h^{-1}. (For interpretation of the references to color in this figure legend, the reader is referred to the web version of this article.)

Fig. 2. NO$_x$ reduction results from fixed powder bed micro-reactor experiments using pure EtOH as reducing agent at a C/N molar ratio of 3. Left panel: Ag2 (red) and Ag4 (blue), right panel: Ag2Pt100 (black) and AgPt500 (green). Inlet gas composition: 500 ppm NO, 10 vol.% O$_2$, 5 vol.% H$_2$O, and N$_2$ balance; GHSV = 50,000 h^{-1}. (For interpretation of the references to color in this figure legend, the reader is referred to the web version of this article.)
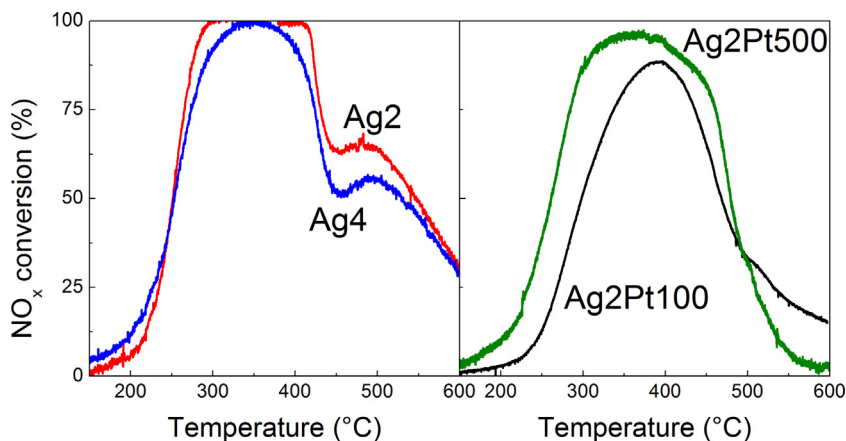

Fig. 3. NO$_x$ reduction results from fixed powder bed micro-reactor experiments using equal C$_1$ molar amounts of EtOH and C$_3$H$_6$ as reducing agent at a combined C/N molar ratio of 6. Left panel: Ag2 (red) and Ag4 (blue), right panel: Ag2Pt100 (black) and AgPt500 (green). Inlet gas composition: 500 ppm NO, 10 vol.% O$_2$, 5 vol.% H$_2$O, and N$_2$ balance; GHSV = 50,000 h^{-1}. (For interpretation of the references to color in this figure legend, the reader is referred to the web version of this article.)

ated using ethanol/gasoline blends as reducing agent: E100 (100% EtOH), E85 (85% EtOH—15% gasoline) and E50 (50% EtOH—50% gasoline). The blends were prepared in-house by mixing 100% ethanol (Decon Laboratories) and EEE-Lube Certification Gasoline (Haltermann Solutions) in order to ensure correct concentrations.

The synthetic bench-scale gas flow reactor consisted of a quartz tube encased in a tube furnace (Lindberg Blue/M) [12]. The monolith sample was wrapped with thermally cleaned fiberglass strands and placed at the outlet of the reactor chamber. Three thermocouples (type K) were placed inside the reactor chamber close
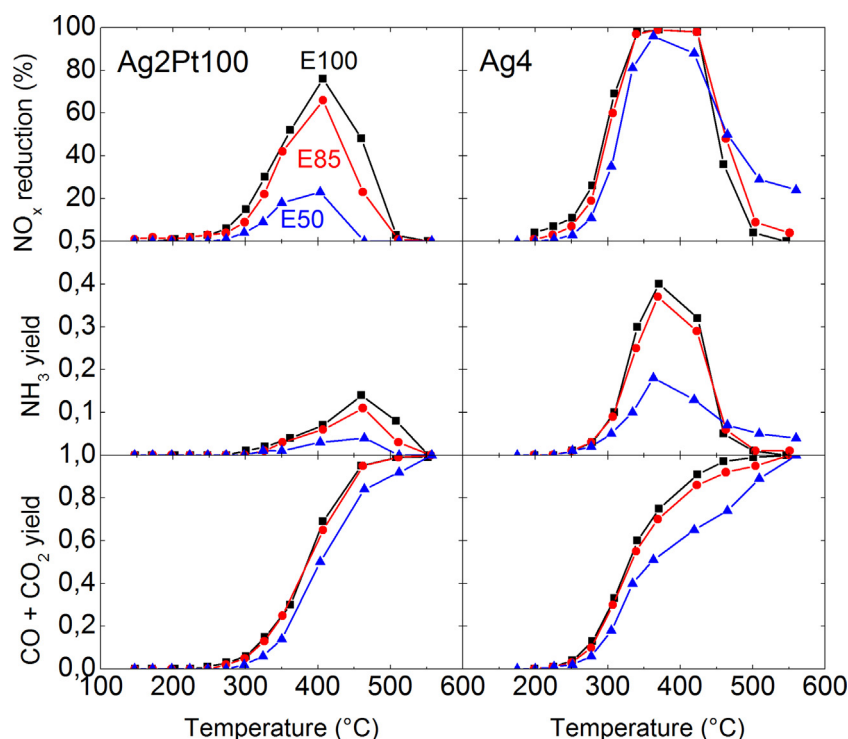
Fig. 4. NO_x reduction results (top panels), NH_3 yield (middle panels) and $CO + CO_2$ yield (bottom panels) from synthetic gas flow reactor experiments for 2 wt.% Ag/Al_2O_3 with 100 ppm Pt (left panels) and 4 wt.% Ag/Al_2O_3 (right panel) using EtOH/gasoline blends as reducing agent. Blends are denoted as E100 (■), E85 (●) and R50 (▲). Inlet gas composition: 500 ppm NO, 10 vol.% O_2, 5 vol.% H_2O, and N_2 balance. The C/N molar ratio was 6 and GHSV = 35,000 h^{-1}.

to the monolith; 5 mm upstream, 5 mm downstream, and at the midpoint of the catalyst sample. The quartz tube was filled with 3 mm quartz beads upstream of the monolith, ensuring a uniform temperature profile of the gases. The inlet gas concentration was controlled by separate mass flow controllers (MKS Instruments) and the outlet gas composition was analyzed using an FTIR gas-analyzer (MKS 2030 HS). Water was introduced using a custom vapor delivery system consisting of an HPLC pump (Eldex Laboratories), which introduced the liquid to a 200 °C inert gas feed *via* a stainless steel capillary. The capillary was wrapped around a heating cartridge, prior to being introduced to the gas. The reducing agent was introduced by a syringe pump (Chemyx) through a stainless steel capillary into a preheated inert carrier gas stream. All tubing up-stream of the reactor was heated to approximately 200 °C in order to ensure no condensation of liquid reactants, while preventing reactions prior to the reactor.

2.3. Surface species analysis

The evolution of surface species on the sample during reaction conditions was followed in situ using a Harrick Scientific ellipsoidal mirror diffuse reflection infrared Fourier transformed spectroscopy (DRIFTS) accessory coupled to a MIDAC model M2500 FTIR spectrometer [26]. The DRIFTS reactor was comprised of a double fast-switch inlet, connected to separate mass flow controllers, enabling fast changes in the reaction conditions. In addition, two temperature-controlled water-baths enabled the introduction of vaporized EtOH and H_2O. The reactor cell consisted of a dome-shaped zinc selenide (ZnSe) window positioned over a brushed aluminum sample holder with the catalyst powder samples lightly covering the aluminum. The sample holder was kept in place by a bent thermocouple, simultaneously monitoring the temperature with high accuracy. The samples were initially pre-treated at 500 °C in 10% O_2 and 5% H_2O, where after the temperature was decreased in 50 °C steps to record background spectra while still flowing O_2

and H_2O. This procedure continued down to 150 °C, where the first spectra were recorded. Initially a time-resolved storage experiment was performed with one measurement every minute, where after further spectra were recorded until surface saturation was ensured. Subsequently the temperature was increased to the next corresponding background temperature and spectra were recorded after saturation was reached.

3. Results and discussion

The Ag powder catalysts were initially evaluated using a fixed bed micro-reactor in order to validate their efficiency for NO_x reduction and to provide a basis for further studies. The catalysts were evaluated using both pure EtOH and an 1:1 mixture of EtOH and C_3H_6, as reducing agent. Based on the experiments with powder samples, and on data acquired using commercial biodiesel, showing that samples doped with trace amounts of platinum exhibit an extended operating temperature window maintaining a higher NO_x reduction compared to the pure Ag-sample [19], the Ag4 and Ag2Pt100 samples were selected for further evaluation. The samples were wash-coated onto cordierite monoliths and evaluated in a continuous gas flow bench-scale reactor. The reductant used was an in-house mixture of EtOH and gasoline (EEE-Lube Cert Gasoline), corresponding to E100, E85 and E50 [12]. Finally, the Ag2 and Ag2Pt500 catalysts were evaluated using DRIFTS, in an attempt to capture the effect of the platinum addition.

3.1. Evaluation of NO_x reduction over model powder catalysts

Activity studies in micro-reactor were performed for four powder samples; three 2 wt.% Ag/Al_2O_3 catalysts, with 0, 100 and 500 ppm Pt, and one 4 wt.% Ag/Al_2O_3 sample. The experiments were performed at three different conditions: pure EtOH with a C/N ratio of 6 (1500 ppm EtOH, Fig. 1) or 3 (750 ppm EtOH, Fig. 2), as well as a 1:1 mixture of EtOH and C_3H_6 with a C/N ratio of 6 (750 ppm

Table 1
Surface species with wavenumbers and references.

Species	Wavenumber	Site	Reference
CHO species			
bidentate carbonate	1620–1530, 1270–1250	Me/oxide	[37]
	1680–1530, 1440–1320	Me/oxide	[38]
monodentate carbonate	1530–1470, 1370–1300	Me/oxide	[37]
	1550–1480, 1410–1340	Me/oxide	[38]
Formate	1590, 1390, 1378	Al_2O_3	[39]
	3005, 2910, 1595, 1390, 1380, 1375	Al_2O_3, Ag/Al_2O_3	[40,41]
	1390, 1376	Al_2O_3	[42]
	1392, 1377	Ag/Al_2O_3	[34,43]
acetate	1580–1570, 1465–1460	Ag/Al_2O_3	[39,42,44]
	1570, 1466, 1394	Ag/Al_2O_3	[45]
	1590–1550, 1465, 1355	Al_2O_3	[42]
acetate or free carboxylate species	1576, 1458	Ag/Al_2O_3	[34,43,46]
acrylate species	1645, 1570, 1455, 1392–1378, 1297	Ag/Al_2O_3	[34,35]
(ethyl) carbonate	1630, 1412, 1340	Ag/Al_2O_3	[41]
	1626, 1412, 1336	Ag/Al_2O_3	[44]
enolic species	1633, 1416, 1336	Ag/Al_2O_3	[36]
	1630, 1412, 1333	Ag/Al_2O_3	[45]
NOx species			
monodentate nitrate	1530–1480, 1290–1250	Me/oxide	[47]
	1560, 1558, 1556, 1550, 1297, 1250, 1245	Ag/Al_2O_3	[32,33,36]
bidentate nitrate	1565–1500, 1300–1260	Me/oxide	[47]
	1590, 1586, 1585, 1304, 1298, 1295, 1248	Ag/Al_2O_3	[32,33,36]
bridging nitrate	1650–1600, 1225–1170	Me/oxide	[47]
	1615, 1614	Ag/Al_2O_3	[32,33,36]
nitrosonium ion (NO+)	2311–2237	Ag/Al_2O_3	[35]
-NCO/-CN species			
-NCO	2255 (Al(VI)-NCO), 2228 (Al(IV)-NCO)	Ag/Al_2O_3	[41]
	2232 (Ag+-NCO)	Ag/Al_2O_3	[43]
	2230	Al_2O_3, Ag/Al_2O_3	[40]
	2229	Ag/Al_2O_3	[45]
-CN	2155, 2127	Ag/Al_2O_3	[41]
	2162, 2130	Ag/Al_2O_3	[43]
	2135	Al_2O_3, Ag/Al_2O_3	[40]

EtOH + 500 ppm C_3H_6, Fig. 3). The C/N molar ratio, *i.e.* 3 and 6, were chosen in order to mimic relevant reaction conditions, still keeping the fuel penalty as low as possible [11]. The experiments with pure EtOH as reducing agent, C/N = 6 (Fig. 1), show similar light-off performance for the Ag2 and Ag4 samples, reaching full NO_x reduction (>98%) at 300 °C. The reduction over the Ag4 sample starts to decrease at 410 °C, whereas the reduction over the Ag2 sample remains above 95% up to 470 °C. Above 510 °C the NO_x reduction is similar for both samples. For the Pt doped (Ag2Pt100 and Ag2Pt500) samples, the light-off performance is similar reaching full reduction at 325 °C. The NO_x reduction over the Ag2Pt500 sample starts to decrease already at 365 °C, whereas for the Ag2Pt100 sample the reduction remains high up to 470 °C. The decrease at lower temperatures for the higher Pt content suggests that the direct oxidation of the reductant with O_2 is more efficiently catalyzed at these temperatures.

When the EtOH concentration is decreased to a C/N molar ratio of 3 (Fig. 2), the differences between the pure Ag samples become more prominent. The Ag2 sample displays full NO_x reduction (>99%) between 290–390 °C, whereas the Ag4 sample only reaches a maximum reduction of 80% at 330 °C. For the Pt doped samples, the light-off performance is identical up to 310 °C, where after the reduction over the Ag2Pt500 sample levels out and follows a typical volcano shape with reductions above 92% between 325 and 370 °C. The Ag2Pt100 sample displays full NO_x reduction (>98%) between 340 and 405 °C, followed by a steep decrease above 410 °C. Additional experiments with a mixed reducing agent (equimolar amounts of EtOH and C_3H_6) and C/N = 6 (Fig. 3) were performed in order to simulate ethanol/gasoline blends, as such fuels are commercially available on a large scale. For the pure Ag samples, the Ag2 is again the catalyst which displays the highest NO_x reduction over

the broadest temperature window reaching >98% between 290 and 415 °C. Also for the Ag4 sample full reduction (>98%) is reached, however only between 325 and 375 °C. For the platinum doped samples, the Ag2Pt500 sample displays an overall higher reduction compared to the Ag2Pt100 sample, reaching a maximum of >95% between 325 and 395 °C, potentially owing to the platinum's ability to partially oxidize the C_3H_6. For the Ag2Pt100 sample however, only a reduction of >87% is reached, this between 375 and 405 °C. The dual peak performance for the pure silver samples (seen in Fig. 3) is likely related to accumulation of propene at low temperature. While ethanol is an efficient reductant also in the low temperature regime, propene does not start to reduce NO_x until around 400 °C over this type of system [17]. At higher temperature, propene desorbs and improves the NO_x reduction. This behaviour is more obvious for the silver alumina sample compared to the Pt doped sample as Pt has higher activity to promote the oxidation reactions compared to silver. Hence, the desorbed propene is combusted by molecular oxygen, rather than reacting with the NO_x, to a higher extent for the Pt doped sample compare to the pure silver sample.

In summery the Ag2 sample displays the highest overall NO_x reduction over the broadest temperature interval of the pure Ag samples investigated. The platinum doped samples generally display a lower overall reduction compared to the pure Ag samples, however extended towards higher temperatures. Hence, one doped and one pure Ag-alumina catalyst sample are selected to be evaluated after being wash-coated on monolith substrates, using in-house mixed gasoline/EtOH as reducing agent. As previous studies have shown that higher silver loadings are necessary when more complex hydrocarbons are used as the reductant [20]; the

catalysts chosen for these experiments were the Ag4 and the Ag2Pt100 sample.

3.2. Evaluation of NO_x reduction over monolith catalysts with complex reducing agents

As stated previously, the Ag4 and Ag2Pt100 samples were wash-coated onto monoliths substrates and the NO_x reduction over these samples was evaluated at steady state conditions with an ethanol/gasoline blend as the reducing agent. The results are illustrated in Fig. 4 with NO_x reduction (top panels), NH_3 formation (middle panels) and $CO + CO_2$ yield (bottom panels). The results show a much higher NO_x reduction and NH_3 formation over the pure 4 wt.% Ag sample (Ag4) compared to the 100 ppm Pt doped 2 wt.% Ag sample (Ag2Pt100), with the Ag4 sample displaying a light-off in NO_x reduction at approximately 50 °C lower temperature then the Ag2Pt100 sample. In addition, the E85 and E100 results show very similar reduction for the Ag4 sample, whereas the E100 shows strictly higher reduction than E85 over the Ag2Pt100 sample. The results with E50 over the Ag4 sample displays slightly lower reduction at temperatures below 450 °C compared to E85 and E100. However, above 450 °C, employing E50 as the reductant results in higher reduction thanks to that the gasoline constituents are more difficult to oxidize compared to EtOH, but the overall reactivity is still too low to be significant. The results for the Ag2Pt100 sample using E50, do not show any improvements at high temperatures, but instead an overall decrease in NO_x reduction is observed as the Pt appears to facilitate the oxidation of the gasoline components. The HC conversion, derived from the formation of CO and CO_2, is almost identical when comparing E100 and E85 for the two catalysts individually. Further, the HC light-off over the Ag4 sample starts at approximately 50 °C lower temperature compared to the Ag2Pt100 sample correlating with the light-off profile in NO_x reduction. The overall reduction is considerably lower than that of the pure Ag samples. The experiments performed using the coated monolith samples (Fig. 4), using EtOH/gasoline blends, resemble those using the EtOH/C_3H_6 mixture, with a lower NO_x reduction for the Pt doped samples as compared to the pure Ag samples. The NO_x reduction over the Pt doped samples does, however, show a substantial decrease when the gasoline content is increased, whereas the NO_x reduction over the pure Ag samples remains high, with the
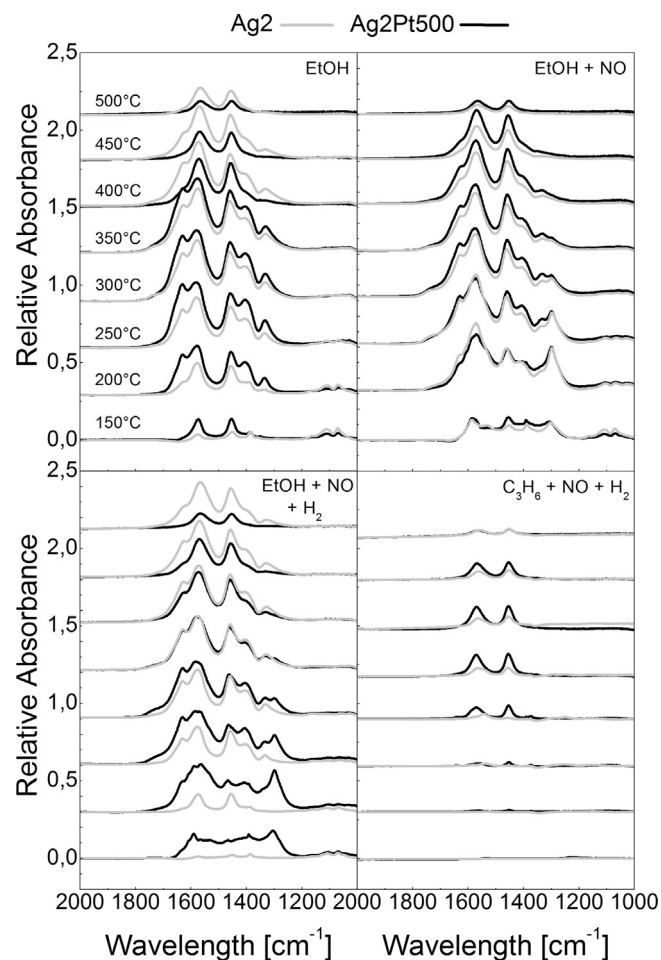

Fig. 5. Temperature resolved DRIFTS absorption spectra over Ag2 (gray) and Ag2Pt500 (black) samples with argon and oxygen balance. Specific compounds are: ethanol (top left); ethanol and NO (top right); ethanol, NO and hydrogen (bottom left); and propene, NO and hydrogen (bottom right).
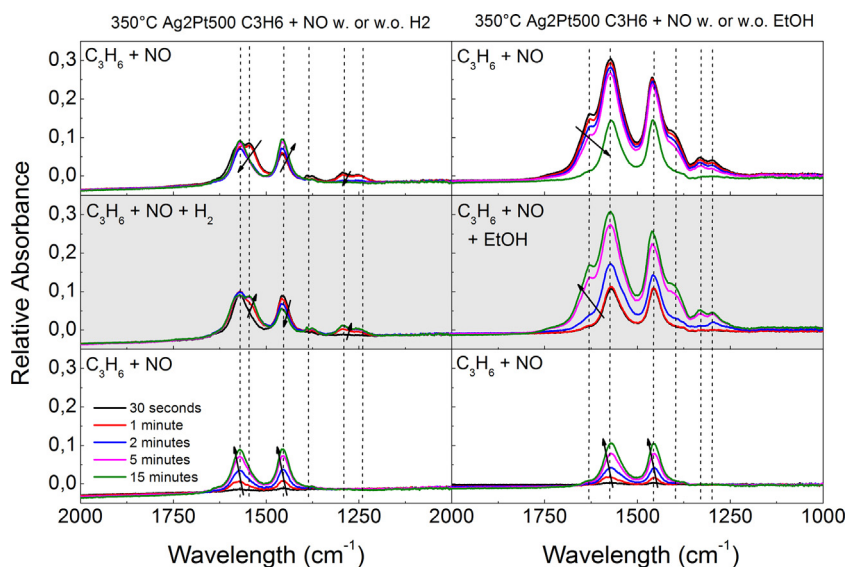

Fig. 6. Comparing formation/desorption over Ag2Pt500 samples. Initially C_3H_6, NO, O_2 with argon balance depicted in the bottom two panels. The second row shows the addition of hydrogen (left hand) or ethanol (right hand), followed by removal of these compounds in the top row.

high-temperature activity increasing with increasing gasoline concentration. This is most likely related to the small silver species in these samples favoring NO_x reduction rather than hydrocarbon oxidation reactions. Alternatively, this could be a result of the higher binding energy of hydrocarbon to Pt compared to Ag [27] as well as a potential selective poisoning from aromatic compounds in the gasoline [28], which would be higher for the platinum containing species [27]. Furthermore, the NH_3 formation is considerably higher over the Ag4 sample compared to the Ag2Pt100 sample. At low levels the formation of NH_3 is considered an unwanted by-product, however at the levels showed here it is possibly an asset. Combining a system of this type with an NH_3-SCR catalyst that has a considerable NH_3 storage capacity, could very well result in an interesting dual SCR system [12,13]. As stated in the introduction, the addition of urea tanks in light-duty vehicles is undesirable due to handling problems and space limitation, hence NH_3-SCR has been considered as a heavy-duty technology only. In addition, one key challenge with HC-SCR is high NO_x reduction while minimizing the fuel penalty derived from the hydrogen reformation of the fuel and the consumption of fuel as reducing agent. As the EtOH-SCR does not require H_2 in order to achieve high NO_x reduction [12], this contribution to the fuel penalty is avoided. If the EtOH-SCR system would be connected to a down-stream NH_3-storage/SCR catalyst, the produced ammonia could be utilized for NO_x reduction. Supplying the EtOH transiently to the Ag alumina catalyst could result in a cycling between HC-SCR, reducing NO_x and charging the NH_3-storage/SCR catalyst, followed by a NH_3-SCR, reducing NO_x and consuming the stored ammonia. This could reduce the fuel penalty even further.

3.3. Evolution of surface species during reaction over model catalysts

In order to acquire more information on the reaction mechanism and the difference between pure Ag and Pt doped Ag samples, the Ag2 and Ag2Pt500 samples were investigated using DRIFTS. The experiments were performed by measuring background spectra at steady state in 50 °C intervals between 500–150 °C in an Ar, O_2 and H_2O atmosphere, followed by the introduction of the investigated species subsequently stepping up the temperature from 150 to 500 °C, and subtracting the corresponding background spectra. Absorption bands and the assignment of the corresponding surface species are summarized in Table 1.

The results show a significant difference in the absorption behaviour for the pure and the Pt-doped Ag/Al_2O_3 samples for most reactants (Fig. 5). For the experiments using EtOH or EtOH, NO, and H_2, the Pt doped sample displays more intense absorption peaks below 400 °C (especially at 150 and 200 °C), while the pure Ag sample displays stronger absorption bands above 400 °C. This corroborates previous studies [19] where the platinum was thought to increase the adsorption of the reactants on the catalyst surface at low temperatures. Curiously, using only EtOH and NO the absorption bands for both samples (Pt-doped and pure Ag) are quite similar, with the doped sample displaying slightly higher peaks above 300 °C compared to the pure Ag sample. A similar trend is seen for the experiments with C_3H_6 + NO + H_2, with less absorption peaks for the Ag2 sample and clearly more intense absorption for the Ag2Pt500 sample between 300 and 450 °C. Importantly, the overall number of surface species is significantly muted for this case without EtOH, particularly with respect to absorption due to nitrate related surface species (key indicator is near 1300 cm^{-1} [29–33]). This highlights the importance of ethanol to facilitate NO_x adsorption and initial reactivity. Regarding the other absorption peaks, no large variation in peaks is observed for the two catalytic samples.

As stated previously, the possible correlation between ethanol and formation of surface hydrogen was also studied. It has been
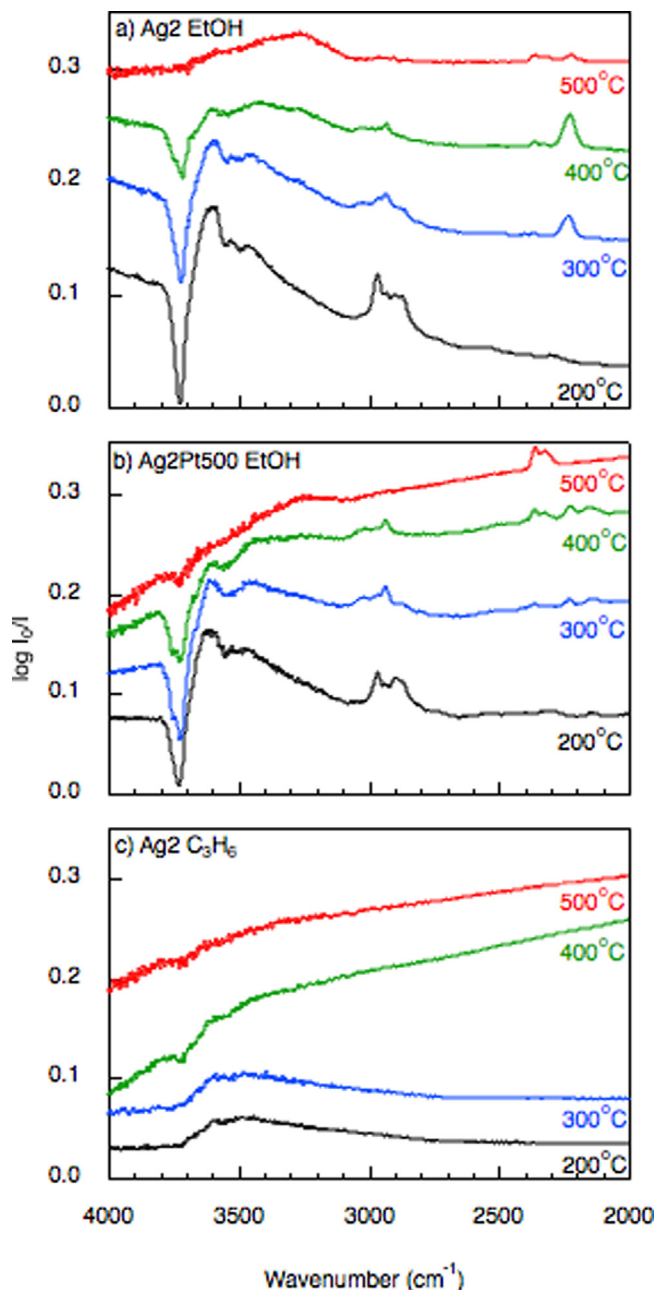

Fig. 7. Temperature resolved DRIFTS absorption spectra showing the isocyanate and ammonia regions for a) the Ag2 sample with ethanol, NO and O_2, b) the Ag2Pt500 sample with ethanol, NO and O_2, and c) the Ag2 sample with C_3H_6, NO and O_2 (Ar bal.).

suggested that the OH-group in EtOH could act as a hydrogen source, explaining the absence of the promotional effect from hydrogen addition on the NO_x reduction when using EtOH as the reducing agent. This has previously been shown for methanol-SCR over similar types of silver samples [48]. In order to investigate this hypothesis, data from NO reduction experiments using C_3H_6 + NO + O_2 (Ar balance), were performed, while introducing either H_2 or EtOH, keeping the C/N ratio constant (Fig. 6). When neither H_2 nor EtOH are present in the feed, the intensity of the peaks at 1577–1571 and 1454 cm^{-1} increases with time, likely representing the build-up of acrylate and/or acetate species on the surface of the catalyst. The intensity of the absorption due to these species remain fairly constant when H_2 is introduced to the feed, with a slight shift towards lower wavenumbers (Fig. 6, left mid-

dle panel). The shift near 1550 cm^{-1} is likely related to the peak growing at 1300 cm^{-1}, which, as listed in Table 1 and discussed earlier, is associated with nitrate formation (1550 and 1300 cm^{-1}). This indicates increased reactivity of the NO$_x$ with H$_2$ and subsequently increased presence of nitrogen-containing species on the surface. Other small peaks at 1250, 1376, and 1390 cm^{-1} are also observed, likely owing to the formation of acrylate, acetate, formate and/or carbonates. It is clear that the number of different surface species and their intensity is considerably higher when EtOH is used as reducing agent as compared to the H$_2$-assisted C$_3$H$_6$ (Fig. 6, right middle panel). New peaks are observed at 1295, 1330, ~1400 and 1629 cm^{-1}, indicating formation of nitrates, acrylates, enolic species, and formate on the surface. Männikkö et al. [48] observed formation of formate species on a silver alumina surface during methanol oxidation experiments, while for the same conditions mainly methoxy species where formed over the corresponding alumina surface. The authors suggested a reaction route where the formate species were formed from surface methoxy species, *via* release of hydrogen atoms, that subsequently form H$_2$ and/or H$_2$O. The as formed hydrogen is proposed to have a similar role for the NO$_x$ reduction as the corresponding added gaseous hydrogen, *i.e.* H$_2$. It is highly likely that this route is also applicable for ethanol oxidation over a silver alumina catalyst.

In addition, peaks in the range of 2235–2225 cm^{-1}, related to surface bound isocyanate species, are observed for the EtOH and NO experiments (Fig. 7a–b), however these peaks are not present for experiments with propene and NO (Fig. 7c). Previous studies have suggested that isocyanate species are possible reaction intermediates in the formation of ammonia [45–47]. It has also been demonstrated that such NCO surface species can readily react with water forming NH$_3$, see *e.g.* [49]. In Fig. 7 it can clearly be seen that NCO surface species mainly are formed over the pure silver sample and to a lower degree over the platinum doped sample. Formation of surface bound ammonia, shown as peaks in the region around 3300–3400 cm^{-1} [49], also occurs to a higher degree over the pure silver sample (Fig. 7a) compared to the platinum doped one (Fig. 7b), corroborating the lower NH$_3$ formation seen in gas phase over the Ag2Pt100 sample.

4. Concluding remarks

This study shows a high activity for NO$_x$ reduction over sol-gel synthesized Ag/Al$_2$O$_3$ catalysts when using EtOH and EtOH/gasoline blends as reducing agents for NO$_x$. Although platinum doping displays some improvements in activity during the powder reactor experiments, this improvement is not transferable to the EtOH/gasoline results for monolith samples. One explanation to this is the different residence time for the powder and monolith experiments, and potentially also an effect of increased surface adsorption of aromatic compounds from the gasoline at low temperatures, which poisons the catalyst surface. The 4% Ag/Al$_2$O$_3$ sample shows a higher reduction, lower onset temperature and higher NH$_3$ formation, for all three EtOH/gasoline mixtures compared to the 2% Ag/Al$_2$O$_3$ sample doped with 100 ppm Pt. The high formation of NH$_3$ is related to the higher formation of isocyanates for the pure Ag sample compared to the Pt doped sample, and shows promising implication for further studies. In combination with a NH$_3$-storage/SCR catalyst system, which could result in a decreased fuel penalty, the silver-alumina catalyst provides an efficient NO$_x$ reduction system for ethanol powered vehicles.

Disclaimer

Acknowledgments

References

[1] R. Detels, D.P. Tashkin, J.W. Sayre, S.N. Rokaw, F.J. Massey, A.H. Coulson, D.H. Wegman, Am. J. Public Health 81 (1991) 350.
[2] D. Price, R. Birnbaum, R. Batiuk, M. McCullough, R. Smith, Nitrogen oxides: Impacts on public health and the environment, Other Information: PBD: Aug 1997, 1997, pp. Medium: P; Size: 165 p.
[3] C. European Parliament, Regulation (EC) No 715/2007 (2007).
[4] S.I. Matsumoto, CATTECH 4 (2000) 102.
[5] K. Skalska, J.S. Miller, S. Ledakowicz, Sci. Total Environ. 408 (2010) 3976.
[6] K. Arve, J.R.H. Carucci, K. Eränen, A. Aho, D.Y. Murzin, Appl. Catal. B 90 (2009) 603.
[7] K. Arve, K. Eränen, M. Snåre, F. Klingstedt, D. Murzin, Top. Catal. 42–43 (2007) 399.
[8] S. Satokawa, Chem. Lett. 29 (2000) 294.
[9] T. Miyadera, Appl. Catal. B 2 (1993) 199.
[10] R. Burch, J.P. Breen, C.J. Hill, B. Krutzsch, B. Konrad, E. Jobson, L. Cider, K. Eranen, F. Klingstedt, L.E. Lindfors, Top. Catal. 30–31 (2004) 19.
[11] H. Kannisto, X. Karatzas, J. Edvardsson, L.J. Pettersson, H.H. Ingelsten, Appl. Catal. B 104 (2011) 74.
[12] J.A. Pihl, T.J. Toops, G.B. Fisher, B.H. West, Catal. Today 231 (2014) 46.
[13] G.B. Fisher, C.L. DiMaggio, D. Trytko, K.M. Rahmoeller, M. Sellnau, SAE Int. J. Fuels Lubr. 2 (2009) 313.
[14] Y. Itoh, M. Ueda, H. Shinjoh, M. Sugiura, M. Arakawa, J. Chem. Technol. Biotechnol. 81 (2006) 544.
[15] C.K. Narula, C.S. Daw, J.W. Hoard, T. Hammer, Int. J. Appl. Ceram. Technol. 2 (2005) 452.
[16] H. Kannisto, H. Ingelsten, M. Skoglundh, Top. Catal. 52 (2009) 1817.
[17] H. Kannisto, K. Arve, T. Pingel, A. Hellman, H. Harelind, K. Eranen, E. Olsson, M. Skoglundh, D.Y. Murzin, RSC Catal. Sci. Technol. 3 (2013) 644.
[18] M. Männikkö, M. Skoglundh, H.H. Ingelsten, Appl. Catal. B 119–120 (2012) 256.
[19] F. Gunnarsson, H. Kannisto, M. Skoglundh, H. Härelind, Appl. Catal. B 152–153 (2014) 218.
[20] F. Gunnarsson, J.-Y. Zheng, H. Kannisto, C. Cid, A. Lindholm, M. Milh, M. Skoglundh, H. Härelind, Top. Catal. 56 (2013) 416.
[21] H. Kannisto, H.H. Ingelsten, M. Skoglundh, J. Mol. Catal. A 302 (2009) 86.
[22] F. Gunnarsson, M.Z. Granlund, M. Englund, J. Dawody, L.J. Pettersson, H. Härelind, Appl. Catal. B 162 (2015) 583.
[23] Y. Ji, T.J. Toops, M. Crocker, Catal. Lett. 119 (2007) 257.
[24] T.J. Toops, B.G. Bunting, K. Nguyen, A. Gopinath, Catal. Today 123 (2007) 285.
[25] T.J. Toops, J.A. Pihl, Catal. Today 136 (2008) 164.
[26] T.J. Toops, D.B. Smith, W.P. Partridge, Appl. Catal. B 58 (2005) 245.
[27] T. Bligaard, J.K. Nørskov, S. Dahl, J. Matthiesen, C.H. Christensen, J. Sehested, J. Catal. 224 (2004) 206.
[28] V. Demidyuk, C. Hardacre, R. Burch, A. Mhadeshwar, D. Norton, D. Hancu, Catal. Today 164 (2011) 515.
[29] S. Kameoka, Y. Ukisu, T. Miyadera, Phys. Chem. Chem. Phys. 2 (2000) 367.
[30] H.H. Ingelsten, A. Hellman, H. Kannisto, H. Grönbeck, J. Mol. Catal. A 314 (2009) 102.
[31] S. Tamm, H.H. Ingelsten, A.E. Palmqvist, J. Catal. 255 (2008) 304.
[32] A. Iglesias-Juez, A.B. Hungria, A. Martinez-Arias, A. Fuerte, M. Fernandez-Garcia, J.A. Anderson, J.C. Conesa, J. Soria, J. Catal. 217 (2003) 310.
[33] X. Zhang, Y. Yu, H. He, Appl. Catal. B 76 (2007) 241.
[34] Y. Yu, X. Zhang, H. He, Appl. Catal. B 75 (2007) 298.
[35] C. Morterra, G. Magnacca, Catal. Today 27 (1996) 497.
[36] K. Shimizu, H. Kawabata, A. Satsuma, T. Hattori, J. Phys. Chem. B 103 (1999) 5240.

[37] F.C. Meunier, J.P. Breen, V. Zuzaniuk, M. Olsson, J.R.H. Ross, J. Catal. 187 (1999) 493.
[38] N. Bion, J. Saussey, M. Haneda, M. Daturi, J. Catal. 217 (2003) 47.
[39] A. Satsuma, K. Shimizu, Progress Energy Combust. Sci. 29 (2003) 71.
[40] K. Shimizu, J. Shibata, H. Yoshida, A. Satsuma, T. Hattori, Appl. Catal. B 30 (2001) 151.
[41] K. Shimizu, A. Satsuma, T. Hattori, Appl. Catal. B 25 (2000) 239.
[42] H. He, C.B. Zhang, Y.B. Yu, Catal. Today 90 (2004) 191.
[43] F.C. Meunier, V. Zuzaniuk, J.P. Breen, M. Olsson, J.R.H. Ross, Catal. Today 59 (2000) 287.
[44] K.I. Hadjiivanov, Catal. Rev. 42 (2000) 71.
[45] F. Can, X. Courtois, S. Royer, G. Blanchard, S. Rousseau, D. Duprez, Catal. Today 197 (2012) 144.
[46] M.L. Unland, J. Catal. 31 (1973) 459.
[47] D. Zhao, H.H. Ingelsten, M. Skoglundh, A. Palmqvist, J. Mol. Catal. A 249 (2006) 13.
[48] M. Männikkö, X. Wang, M. Skoglundh, H. Härelind, Appl. Catal. B 180 (2016) 291.
[49] H.H. Ingelsten, M. Skoglundh, Catal. Lett. 106 (2006) 15.